Numerical Simulation of Macrosegregation in a 535 Tons Steel Ingot with a Multicomponent-Multiphase Model

Kangxin Chen, Wutao Tu and Houfa Shen

Abstract To accurately simulate the formation of macrosegregation, a major defect commonly encountered in large ingots, solidification researchers have developed various mathematical models and conducted corresponding steel ingot dissection experiments for validation. A multicomponent and multiphase solidification model was utilized to predict macrosegregation of steel ingots in this research. The model described the multi-phase flow phenomenon during solidification, with the feature of strong coupling among mass, momentum, energy, and species conservation equations. Impact factors as thermo-solutal buoyancy flow, grains sedimentation, and shrinkage-induced flow on the macroscopic scale were taken into consideration. Additionally, the interfacial concentration constraint relations were derived to close the model by solving the solidification paths in the multicomponent alloy system. A finite-volume method was employed to solve the governing equations of the model. In particular, a multi-phase SIMPLEC (semi-implicit method for pressure-linked equations-consistent) algorithm was utilized to solve the velocity-pressure coupling for the specific multiphase flow system. Finally, the model was applied to simulate the macrosegregation in a 535 tons steel ingot. The simulated results were compared with the experimental results and the predictions reproduced the classical macrosegregation patterns. Good agreement is shown generally in quantitative comparisons between experimental

K. Chen · H. Shen (✉)
School of Materials Science and Engineering, Tsinghua University,
Beijing 100084, People's Republic of China
e-mail: shen@tsinghua.edu.cn

K. Chen
e-mail: chenkx13@mails.tsinghua.edu.cn

W. Tu
SMIC Advanced Technology Research & Development (Shanghai) Corporation,
Shanghai, China

P. Mason et al. (eds.), *Proceedings of the 4th World Congress on Integrated Computational Materials Engineering (ICME 2017)*,
The Minerals, Metals & Materials Series, DOI 10.1007/978-3-319-57864-4_18

results and numerical predictions of carbon, chromium and molybdenum concentration. It is demonstrated that the multicomponent-multiphase solidification model can well predict macrosegregation in steel ingots and help optimize the ingot production process.

Keywords Macrosegregation · Multicomponent · Multiphase modeling · Steel ingots

Introduction

Large ingots are typically used to produce key components in large equipment, which are used in energy and power, metallurgical machinery, transportation, national defense and other fields. Macrosegregation, i.e. the compositional heterogeneity, is a serious defect commonly encountered in large ingots. This compositional heterogeneity usually leads to the non-uniform distribution of microstructure, harms the mechanical properties, and, at its worst, may even result in scrapping the final product. Macrosegregation results from the combined effect of compositional segregation at the microscopic scale and solid-liquid separation at the macroscopic scale. The relative motion of solid phase and liquid phase is mainly caused by such factors as thermo-solutal buoyancy flow, grains sedimentation, shrinkage-induced flow, and deformation of the solid phase skeleton [1, 2]. As macrosegregation cannot be eliminated by the subsequent heat treatment process, it is important to control the formation of macrosegregation during solidification to obtain a less segregated ingot. Due to the high cost of casting large ingots, it is unrealistic to simply use experimental methods to study macrosegregation. Numerical simulation, with the advantages of low cost and high efficiency, has become an important tool for understanding complex solidification processes and macrosegregation of large ingots.

Since the pioneering work of Flemings and Nereo [3] in 1960s, much effort has been devoted to the modeling of macrosegregation. Varieties of mathematical models have been developed to account for such mechanisms as thermal-solutal convection, free equiaxed crystal movement, solidification shrinkage-induced flow [4, 5]. The macrosegregation models commonly used can be divided into single-phase models, two-phase models and multi-phase models according to the number of basic dynamics phases used. Among them, the relatively simple single-phase models, divided into continuum models and volume average models, mainly consider the thermal-solutal buoyancy flow. The two-phase models or multi-phase models, further considering the effect of free equiaxed crystal motion or solid phase deformation on macrosegregation, however, are rather complicated. Numerous applications of macrosegregation models in steel ingots have been reported. Vannier and Combeau [6] utilized a continuum model to simulate macrosegregation of a 65 tons Fe-0.22 wt%C steel ingot, and compared the predictions with measurements of compositions in the center line. Liu et al. [7] adopted

a continuum model to predict macrosegregation in a 360 tons ingot. Tu and coworkers [8] recently developed a multicomponent-multiphase model based on a two phase model previously developed in his research group, and applied the model to investigate a 36 tons Fe-0.51 wt%C-0.006 wt%S steel ingot, which was experimentally investigated by temperature recording and concentration analysis. In this experiment, the macrosegregation maps of carbon and sulphur were obtained based on 1800 component sampling points covering the entire half-section. General macrosegregation patterns in measurements have been reproduced by predictions. Good agreement is shown in quantitative comparisons between measurements and predictions of carbon and sulphur variations along selected positions. For applications in large steel ingot, single-phase models with much simplification, are still commonly used. The use of two-phase models, especially multi-phase models, is relatively rare. There are two factors accounting for this. On one hand, the development of two-phase models or multi-phase models is rather difficult, which hinders their applications to a certain extent. On the other hand, large ingots, due to their large sizes, will cost more computational time and resources with a two-phase or multi-phase model. Thus, applications of multi-phase macrosegregation models in large ingots with experiment validation are of great significance.

In this paper, the multicomponent-multiphase model developed by the authors has been adopted to predict macrosegregation in a 535 tons steel ingot in three dimensions. The ingot has been simplified as a Fe-0.24 wt%C-1.65 wt%Cr-0.39 wt %Mo quaternary alloy system for simulation. For simplicity, the model considers only the primary phase. The predictions have reproduced the classical macrosegregation patterns, including negative segregation at the bottom of the ingot and positive segregation at the top of the ingot. Finally, to quantitatively compare the results of macroscopic segregation prediction and the measured results, the predictions with measurements of compositions along the center line and three transverse sections are compared.

Mathematic Model

In current research, the air phase is further added in previous two-phase model [9] to considerate the solidification shrinkage of the ingot. Firstly, the mass, momentum, and species conservation equations for solid phase and liquid phase are each derived. Then the volume conservation equation is derived to consider the inhaled air phase due to the solidification shrinkage. Further, the energy conservation equation is derived for the solid-liquid mixture system. Besides, a multicomponent alloy system rather than a two alloy system is considered to further investigate the influence of a third or more of the alloy components on macrosegregation. Thus after adding additional solute conservation equations, the interfacial species balance is derived, further obtaining the interfacial concentration constraint relations for the multicomponent alloy system. For simplicity, the model considers only the primary

Table 1 Mathematical equations of the multicomponent-multiphase model

Mass conservation	$\frac{\partial}{\partial t}(g_{\mathrm{s}}\rho_{\mathrm{s}})+\nabla\cdot(g_{\mathrm{s}}\rho_{\mathrm{s}}\boldsymbol{v}_{\mathrm{s}})=\Gamma_{\mathrm{s}}$
	$\frac{\partial}{\partial t}(g_{\mathrm{l}}\rho_{\mathrm{l}})+\nabla\cdot(g_{\mathrm{l}}\rho_{\mathrm{l}}\boldsymbol{v}_{\mathrm{l}})=-\Gamma_{\mathrm{s}}$
Momentum conservation	$\frac{\partial}{\partial t}(g_{\mathrm{s}}\rho_{\mathrm{s}}\boldsymbol{v}_{\mathrm{s}})+\nabla\cdot(g_{\mathrm{s}}\rho_{\mathrm{s}}\boldsymbol{v}_{\mathrm{s}}\boldsymbol{v}_{\mathrm{s}})=-g_{\mathrm{s}}\nabla p+\nabla\cdot(g_{\mathrm{s}}\mu_{\mathrm{s}}\nabla\boldsymbol{v}_{\mathrm{s}})+M_s^d+g_{\mathrm{s}}\rho_{\mathrm{s}}\boldsymbol{g}$
	$\frac{\partial}{\partial t}(g_{\mathrm{l}}\rho_{\mathrm{l}}\boldsymbol{v}_{\mathrm{l}})+\nabla\cdot(g_{\mathrm{l}}\rho_{\mathrm{l}}\boldsymbol{v}_{\mathrm{l}}\boldsymbol{v}_{\mathrm{l}})=-g_{\mathrm{l}}\nabla p+\nabla\cdot(g_{\mathrm{l}}\mu_{\mathrm{l}}\nabla\boldsymbol{v}_{\mathrm{l}})-M_s^d+g_{\mathrm{l}}\rho_{\mathrm{l}}^{\mathrm{b}}\boldsymbol{g}$
Volume conservation	$\Delta V_{\mathrm{a}}=\left(\frac{\rho_{\mathrm{s}}}{\rho_{\mathrm{l}}}-1\right)\sum(V_{\mathrm{cell}}\cdot\Delta g_{\mathrm{s}})$
Species conservation	$\frac{\partial}{\partial t}(g_{\mathrm{s}}\rho_{\mathrm{s}}C_{\mathrm{s},i})+\nabla\cdot(g_{\mathrm{s}}\rho_{\mathrm{s}}\boldsymbol{v}_{\mathrm{s}}C_{\mathrm{s},i})=\nabla\cdot(g_{\mathrm{s}}\rho_{\mathrm{s}}D_{\mathrm{s},i}\nabla C_{\mathrm{s},i})+\frac{S_{\mathrm{V}}\rho_{\mathrm{s}}D_{\mathrm{s},i}}{\delta_{\mathrm{s}}}(C_{\mathrm{s},i}^{*}-C_{\mathrm{s},i})+C_{\mathrm{s},i}^{*}\Gamma_{\mathrm{s}}$
	$\frac{\partial}{\partial t}(g_{\mathrm{l}}\rho_{\mathrm{l}}C_{\mathrm{l},i})+\nabla\cdot(g_{\mathrm{l}}\rho_{\mathrm{l}}\boldsymbol{v}_{\mathrm{l}}C_{\mathrm{l},i})=\nabla\cdot(g_{\mathrm{l}}\rho_{\mathrm{l}}D_{\mathrm{l},i}\nabla C_{\mathrm{l},i})+\frac{S_{\mathrm{V}}\rho_{\mathrm{l}}D_{\mathrm{l},i}}{\delta_{\mathrm{l}}}(C_{\mathrm{l},i}^{*}-C_{\mathrm{l},i})-C_{\mathrm{l},i}^{*}\Gamma_{\mathrm{s}}$
Energy conservation	$\frac{\partial}{\partial t}[(g_{\mathrm{s}}\rho_{\mathrm{s}}c_{\mathrm{ps}}+g_{\mathrm{l}}\rho_{\mathrm{l}}c_{\mathrm{pl}})T_{\mathrm{s(l)}}]+\nabla\cdot[(g_{\mathrm{s}}\rho_{\mathrm{s}}c_{\mathrm{ps}}\boldsymbol{v}_{\mathrm{s}}+g_{\mathrm{l}}\rho_{\mathrm{l}}c_{\mathrm{pl}}\boldsymbol{v}_{\mathrm{l}})T_{\mathrm{s(l)}}]=\nabla\cdot[(g_{\mathrm{s}}\lambda_{\mathrm{s}}+g_{\mathrm{l}}\lambda_{\mathrm{l}})\nabla T_{\mathrm{s(l)}}]+\Gamma_{\mathrm{s}}L$
Interfacial concentration balance	$\frac{S_{\mathrm{V}}\rho_{\mathrm{s}}D_{\mathrm{s},i}}{\delta_{\mathrm{s},i}}(C_{\mathrm{s},i}^{*}-C_{\mathrm{s},i})+C_{\mathrm{s},i}^{*}\Gamma_{\mathrm{s}}+\frac{S_{\mathrm{V}}\rho_{\mathrm{l}}D_{\mathrm{l},i}}{\delta_{\mathrm{l},i}}(C_{\mathrm{l},i}^{*}-C_{\mathrm{l},i})-C_{\mathrm{l},i}^{*}\Gamma_{\mathrm{s}}=0$

phase, neglecting the formation of the secondary phase. The model is numerically solved by a homemade FVM code based on a multi-phase SIMPLEC algorithm.

The conservation equations are summarized in Table 1. In Table 1, t is the time, g is the volume fraction, ρ is the density, Γ is the interfacial phase change rate, v is the velocity, p is the pressure, μ is the viscosity, M_s^d is the drag force coefficient between the solid and liquid, $\boldsymbol{g}$ is the gravitational acceleration, ΔV_a is the volume change due to solidification shrinkage per unit time, V_{cell} is the grid cell volume, Δg_s is the grid cell solid volume fraction change per unit time, C is the concentration, S_v is the interfacial area concentration, D is the mass diffusivity, δ is the interfacial solute diffusion lengths, c_p is the specific heat, T is the temperature, λ is the thermal conductivity, L is the latent heat. The subscripts "s" and "l" refer to solid phase and liquid phase, respectively.

The supplementation relations, including the descriptions of interfacial area concentration, the interfacial concentration diffusion layer length as well as the flow model, and detailed derivations of the model can be found in Refs. [8] and [9].

Results and Discussion

The multicomponent-multiphase model was applied to a 535 tons steel ingot, which was cast to produce the low pressure rotor for nuclear power. The steel ingot was 6.0 m in height and 4.0 m in mean diameter. The composition of the steel ingot with 30Cr2Ni4MoV steel grade is shown in Table 2. The molten metal was poured at 1530 °C. After being stripped out of the mold, the ingot was dissected into slices along the center plane, and the carbon, chromium and molybdenum concentrations were measured along the centerline and three transverse sections. The schematic of the ingot with the cross-section sampling positions is shown in Fig. 1.

In current simulation, the Fe-0.24 wt%C-1.65 wt%Cr-0.39 wt%Mo quaternary alloy system was taken as the simplification of the 30Cr2Ni4MoV steel ingot to predict macrosegregation of the carbon, chromium and molybdenum components. The properties of the steel ingot and mold materials used are listed in Tables 3 and 4. The thermodynamic parameters used for multicomponent alloy solidification calculation are listed in Table 5. Due to the symmetry along the centerline axis, only a quarter of the ingot system was simulated. A 3-D orthogonal grid system consisting of 104544 cells was used and the mesh size was 80 mm × 80 mm × 80 mm. A constant time step of 0.5 s was used for the simulation. The initial temperature for the mold, sleeve, and powder are 25, 25, and 1500 °C. The interfacial heat transfer coefficients of the steel ingot system are listed in Table 6.

Table 2 30Cr2Ni4MoV steel grade (wt%)

C	Cr	Ni	Mo	V	Si	P
0.24	1.65	3.68	0.39	0.15	0.04	0.002

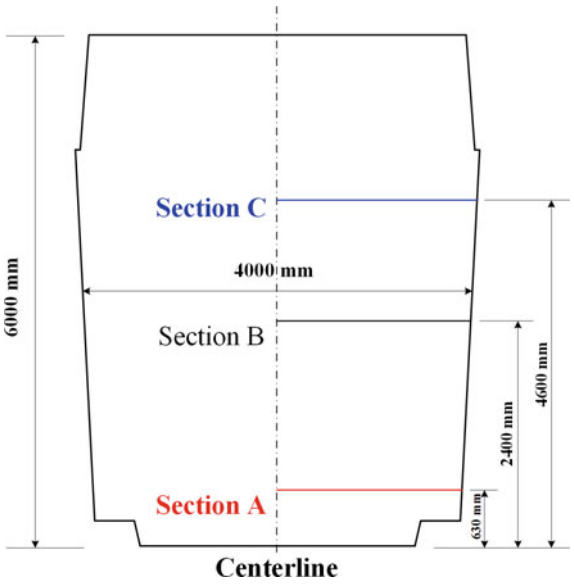

Fig. 1 Schematic of the ingot with the cross-section sampling positions

Table 3 Steel parameters [10, 11]

Property	Value	Unit
Melting temperature of pure iron	1532	°C
Steel thermal expansion coefficient	1.07×10^{-4}	K^{-1}
Liquid density	6990	$kg \cdot m^{-3}$
Solid density	7300	$kg \cdot m^{-3}$
Latent heat	2.71×10^{5}	$J \cdot kg^{-1}$
Liquid viscosity	4.2×10^{-3}	$kg \cdot m^{-1} \cdot s^{-1}$
Thermal conductivity	39.3	$W \cdot m^{-1} \cdot K^{-1}$
Specific heat	500	$J \cdot kg^{-1} \cdot K^{-1}$

Table 4 Thermophysical properties of the mold materials [12]

	Density ($kg \cdot m^{-3}$)	Thermal conductivity ($W \cdot m^{-1} \cdot K^{-1}$)	Specific heat ($J \cdot kg^{-1} \cdot K^{-1}$)
Mold	7000	26.3	540
Sleeve	185	1.4	1040
Powder	260	0.6	1040
Air	1.185	0.026	1000

Table 5 Thermodynamic parameters of Fe-C-Cr-Mo quaternary alloy system

Liquidus temperature (°C)	$1532\text{-}7800 \cdot C\text{-}261 \cdot Cr\text{-}325 \cdot Mo$
Carbon solute partition coefficient	0.34
Chromium solute partition coefficient	0.76
Molybdenum solute partition coefficient	0.56
Carbon solute diffusion coefficient in liquid ($m^2 \cdot s^{-1}$)	2×10^{-8}
Chromium solute diffusion coefficient in liquid ($m^2 \cdot s^{-1}$)	2×10^{-8}
Molybdenum solute diffusion coefficient in liquid ($m^2 \cdot s^{-1}$)	2×10^{-8}
Carbon solute expansion coefficient ($wt\%^{-1}$)	1.10×10^{-2}
Chromium solute expansion coefficient ($wt\%^{-1}$)	3.97×10^{-3}
Molybdenum solute expansion coefficient ($wt\%^{-1}$)	-1.92×10^{-3}

Table 6 Steel ingot system interfacial heat transfer coefficients ($W \cdot m^{-2} \cdot K^{-1}$) [12]

	Ingot	Mold	Sleeve	Powder	Air
Ingot	–	1500	2	400	5
Mold	1500	–	1000	1000	140
Sleeve	2	1000	–	1000	10
Powder	400	1000	1000	–	10
Air	5	140	10	10	–

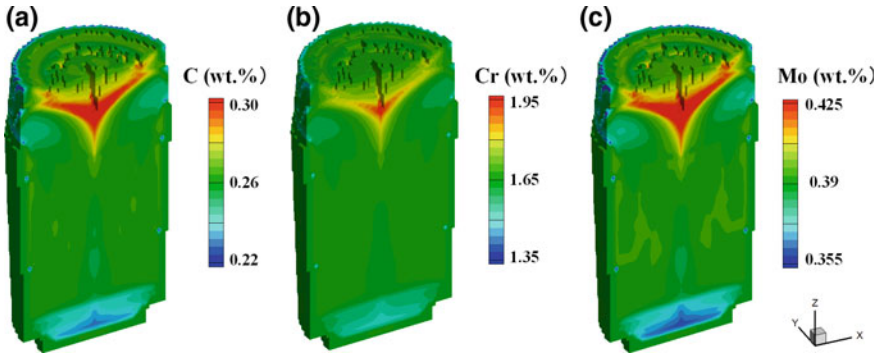

Fig. 2 **a** Predicted carbon concentration, **b** predicted chromium concentration, and **c** predicted molybdenum concentration

The predicted concentration distributions at the end of solidification are shown in Fig. 2a–c. The predicted carbon, chromium, and molybdenum concentrations all exhibit similar patterns, including negative segregation at the bottom of the ingot and positive segregation at the top of the ingot. The predicted macrosegregation patterns for the three components are proven to be qualitatively reasonable.

Quantitative comparisons between predictions and measurements of the solute concentrations along the centerline and three transverse sections A, B and C are provided in Figs. 3 and 4 to evaluate the accuracy of the macrosegregation model. As shown in Fig. 1, the centerline was chosen for its full coverage of the

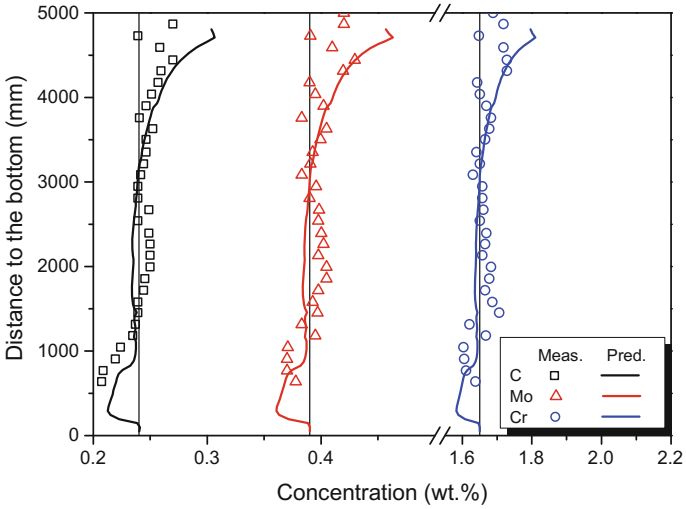

Fig. 3 Concentrations of carbon, chromium and molybdenum along the centerline

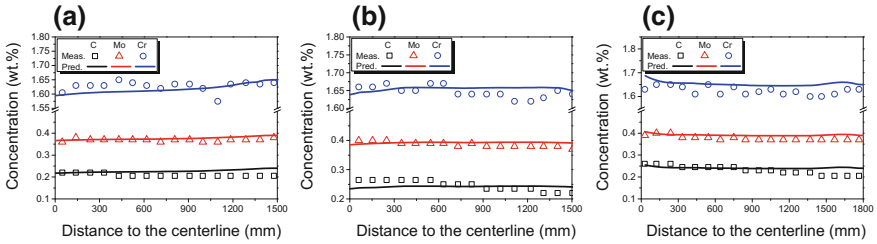

Fig. 4 Concentrations of carbon, chromium and molybdenum along **a** section A, **b** section B and **c** section C

solidification stage of the steel ingot. Section A and Section C, with the height of 630 and 4600 mm, were chosen to represent two typical serious segregation zones in the ingot, i.e. the negative segregation zone due to the sedimentation of solute-lean solid grains and the positive segregation zone formed by solute-rich melt at late stages. Section B, located at the height of 2400 mm over the bottom, represents the concerned ingot body zone. We can see that current predictions are generally in agreement with the measurements. However, for all the three species, some discrepancies arise in the positive segregation zone at the distance to the bottom higher than 3.8 m as shown in Fig. 3. Several factors may contribute to this. Firstly, we have assumed the ingot filling process is instant in the simulation, neglecting the actual multi-pouring process. This simplification ignores the initial non-uniform solute distribution after filling. Secondly, current simulation considers only four components; other components, however, may have a great impact on the solute convection during later stages of solidification [13].

Conclusions

A multicomponent-multiphase model has been applied to investigate the macrosegregation formation in a 535t steel ingot in three dimensions. Typical macrosegregation patterns are reproduced by predictions for carbon, chromium and molybdenum. Moreover, quantitative comparisons between predictions and measurements of the solute concentrations have been made. The results exhibit good agreement except for some discrepancies in the positive segregation zone at the top of the ingot. It is assumed the simplification of the multi-pouring process and ignorance of other components than the Fe-C-Cr-Mo quaternary alloy system may be the main factors.

Acknowledgements This work was financially supported by the NSFC-Liaoning Joint Fund (U1508215) and the project to strengthen industrial development at the grass-roots level of MIIT China (TC160A310/21).

References

1. E.J. Pickering, Macrosegregation in steel ingots: the applicability of modelling and characterisation techniques. ISIJ Int. **53**(6), 935–949 (2013)
2. C. Beckermann, Modelling of macrosegregation: applications and future needs. Int. Mater. Rev. **47**(5), 243–261 (2002)
3. M.C. Flemings, G.E. Nereo, Macrosegregation: part I. Trans. Metall. Soc. AIME **239**(9), 1449–1461 (1967)
4. J. Ni, C. Beckermann, A volume-averaged two-phase model for transport phenomena during solidification. Metall. Trans. B **22**(3), 349–361 (1991)
5. M. Wu, A. Ludwig, A three-phase model for mixed columnar-equiaxed solidification. Metallur. Mater. Trans. A **37**(5), 1613–1631 (2006)
6. I. Vannier, H. Combeau, G. Lesoult, Numerical model for prediction of the final segregation pattern of bearing steel ingots. Mater. Sci. Eng. A **173**(1–2), 317–321 (1993)
7. D.R. Liu et al., Numerical simulation of macrosegregation in large multiconcentration poured steel ingot. Int. J. Cast Met. Res. **23**(6), 354–363 (2010)
8. W.T. Tu et al., Three-dimensional simulation of macrosegregation in a 36-ton steel ingot using a multicomponent multiphase model. JOM **68**(12), 3116–3125 (2016)
9. W.S. Li, H.F. Shen, B.C. Liu, Numerical simulation of macrosegregation in steel ingots using a two-phase model. Int. J. Miner., Metallur. Mater. **19**(9), 787–794 (2012)
10. H. Combeau et al., Prediction of macrosegregation in steel ingots: influence of the motion and the morphology of equiaxed grains. Metallur. Mater. Trans. B **40**(3), 289–304 (2009)
11. L. Thuinet, H. Combeau, Prediction of macrosegregation during the solidification involving a peritectic transformation for multicomponent steels. J. Mater. Sci. **39**(24), 7213–7219 (2003)
12. W.S. Li, Numerical simulation of macrosegregation in large steel ingots based on two-phase model. Ph.D. thesis, Tsinghua University, 2012, pp. 59–103
13. M.C. Schneider, C. Beckermann, Formation of macrosegregation by multicomponent thermosolutal convection during the solidification of steel. Metallur. Mater. Trans. A **9**(26), 2373–2388 (1995)